American Journal of Applied Mathematics
2016; 4(3): 114-123
http://www.sciencepublishinggroup.com/j/ajam
doi: 10.11648/j.ajam.20160403.11
ISSN: 2330-0043 (Print); ISSN: 2330-006X (Online)

Effects of Mass Transfer on Unsteady Hydromagnetic Convective Flow Past an Infinite Vertical Rotating Porous Plate with Heat Source

Thomas Mwathi Ngugi*, Mathew Ngugi Kinyanjui, David Theuri

Department Pure and Applied Mathematics, Jomo Kenyatta University of Agriculture and Technology, Nairobi, Kenya

Email address:

levislinz@gmail.com (T. M. Ngugi)

*Corresponding author

To cite this article:

Thomas Mwathi Ngugi, Mathew Ngugi Kinyanjui, David Theuri. Effects of Mass Transfer on Unsteady Hydromagnetic Convective Flow Past an Infinite Vertical Rotating Porous Plate with Heat Source. *American Journal of Applied Mathematics*. Vol. 4, No. 3, 2016, pp. 114-123. doi: 10.11648/j.ajam.20160403.11

Received: February 11, 2016; **Accepted**: February 23, 2016; **Published**: April 25, 2016

Abstract: The effect of mass transfer on unsteady Hydromagnetic convective flow, of an incompressible electrically conducting fluid, past an infinite vertical rotating porous plate in presence of constant injection and heat source has been investigated. The non-linear partial differential equations governing the flow are solved numerically using the finite differences method. The effect of Hartmann's number, Grashof number for heat transfer, Grashof number for mass transfer, permeability parameter, Schmidt number, Heat source parameter, Prandtl number, Eckert number and rotational parameter on the flow field are presented graphically. A change on the parameters is observed to either increase, decrease or to have no effect on the profiles. The study has some useful information to engineers in the field of oil exploration, geothermal reservoirs, in petroleum and mineral industries, MHD generators, among many other areas.

Keywords: Magnetohydrodynamics (MHD), Porous Medium, Mass Transfer, Heat Source, Injection

1. Introduction

In the past research, researchers have studied a wide variety of flow problems. Subhas et al. (2001) presented a numerical solution of two dimensional laminar boundary layer problems on free convection flow of an incompressible viscous-elastic fluid through a porous medium over a stretching sheet. It was observed among other things that the introduction of chemical species diffusion (modified Grashof number) leads to an increase of horizontal velocity profile either when heating or cooling of the fluid. This observation was found to be true in the presence of porosity parameter but with reduced magnitude. Makinde et al. (2003) discussed the unsteady free convective flow with suction on an accelerating porous plate. Rafael (2005) investigated fluid flow and heat transfer in a porous medium over a stretching surface with internal heat generation and by presence of suction, blowing and impermeability of the surface. He observed that velocity decreases and temperature increases with increasing permeability parameter. He also observed that suction decreases velocity while injection increases the velocity. Kinyanjui et al. (1998) studied the MHD stokes problem for a vertical infinite plate in a dissipative rotating fluid with Hall current and they later investigated the effect of both Hall and Ion-slip currents on the flow of heat generating rotating fluid system. They observed that for an Eckert value of 0.02, there was a decrease in the primary velocity profile with an increase in Rotational parameter. In the case of secondary velocity profiles there is initially a decrease with an increase in Rotational parameter and as the distance from the plate increases, the secondary velocity profile increased. They also observed that an increase in Hall parameter has no effect on the temperature profile but an increase in times causes an increase in the temperature profiles. Das et al. (2006) estimated the mass transfer effects on unsteady flow past an accelerated vertical porous plate with suction employing finite difference analysis. Das et al. (2007) investigated numerically the unsteady free convective MHD flow past an accelerated vertical plate with suction and heat flux. Naser and Elgazery (2008) analyzed numerically

the effects of heat and mass transfer from an isothermal vertical flat plate to a non-Newtonian fluid through a porous medium. It was found that as time approaches infinity, the values of friction factor, heat transfer and mass transfer coefficients approach the steady state values. Das and Mitra (2009) discussed the unsteady mixed convective MHD flow and mass transfer past an accelerated infinite vertical plate with suction. Recently, Das et al. (2009) analyzed the effect of mass transfer on MHD flow and heat transfer past a vertical porous plate through a porous medium under oscillatory suction and heat source. Tamana et al. (2009) analyzed heat transfer in a porous medium over a stretching surface with internal heat generation, suction or injection. They observed that velocity profile decreases with the increase of permeability parameter in both cases of injection and suction. Elbasheshy et al. (2010) studied unsteady boundary layer flow over a porous stretching surface embedded in a porous medium in presence of heat source. He observed that among other things, Nusselt number decreases with increase of porous parameter in the presence of heat source parameter and it also increases with suction. Ferdows et al. (2010) analyzed the problem of heat and mass transfer on natural convection adjacent to a vertical plate in a porous medium with high porosity. They observed that the velocity increases when porous parameter increases and porous parameter has an increasing effect on temperature profiles. Das et al. (2010) investigated the Hydromagnetic convective flow past a vertical porous plate through a porous medium with suction and heat source. Kang'ethe et al. (2012) analyzed various parameters on unsteady MHD laminar boundary layer flow of an incompressible, electrically conducting viscous Newtonian fluids past a stretching sheet embedded in porous media in a rotating system with heat and mass transfer. They concluded among other things that the rate of heat transfer near a stretching surface in a rotating system is influenced by magnitude of the primary velocity profiles rather than by the magnitude of the secondary velocity profiles. They also noted that absence of rotation leads to absence of secondary velocity profiles. Despite the intensive investigation on various areas of MHD by the above mentioned scientists and mathematicians, little has been researched on the effects of mass transfer on unsteady MHD free convective flow past a vertical rotating porous plate in a porous medium with heat source and constant injection.

2. Formulation of the Problem

Consider the unsteady free convective flow of a viscous incompressible electrically conducting fluid past an infinite vertical rotating porous plate in presence of constant injection and heat source and transverse magnetic field. Let the x-axis be taken in vertically upward direction along the plate and y-axis normal to it. The plate is infinite in X-direction and is non-conducting. The fluid and the plate are in a state of rotation about y-axis with uniform angular velocity Ω .The plate is maintained at a uniform temperature T_w . The free stream temperature and concentration are T_∞ and C_∞ respectively. A magnetic field B_0 is applied perpendicular to the plate. Neglecting the induced magnetic field and the Joulean heat dissipation and applying Boussinesq's approximation the governing equations of the flow are given by:

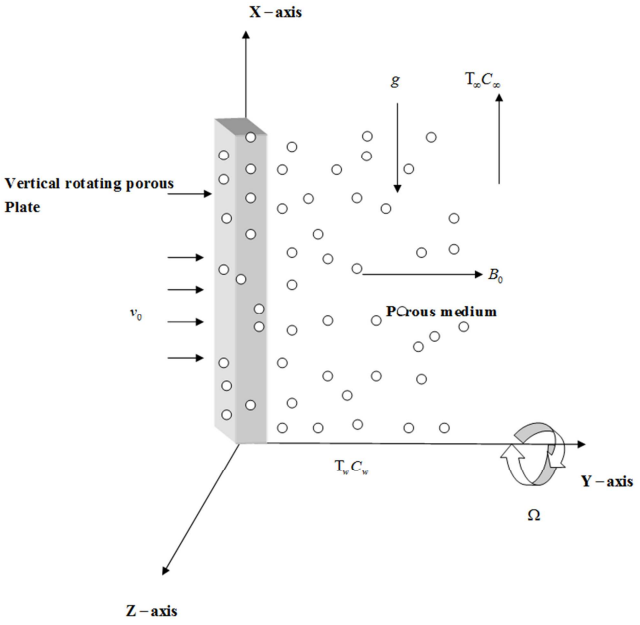

Fig. 1. *Configuration of the problem.*

Continuity equation:

$$\frac{\partial v}{\partial y} = 0 \tag{1}$$

Momentum along x-axis:

$$\frac{\partial u}{\partial t} + v_0 \frac{\partial u}{\partial y} + 2\Omega w = \upsilon \frac{\partial^2 u}{\partial y^2} - \frac{u\upsilon}{k} - \frac{\sigma u B_0^2}{\rho} + gB\left(T - T_\infty\right) + gB^*\left(C - C_\infty\right) \tag{2}$$

Momentum along z-axis:

$$\frac{\partial w}{\partial t} + v_0 \frac{\partial w}{\partial y} + 2\Omega u = \upsilon \frac{\partial^2 w}{\partial y^2} - \frac{w\,\upsilon}{k} - \frac{\sigma w B_0^2}{\rho} \tag{3}$$

Energy equation:

$$\frac{\partial T}{\partial t} + v_0 \frac{\partial T}{\partial y} = \frac{k}{\rho C_p}\frac{\partial^2 T}{\partial y^2} + \frac{\upsilon}{C_p}\left(\frac{\partial u}{\partial y}\right)^2 + \frac{Q_0}{\rho C_p}\left(T - T_\infty\right) \tag{4}$$

Concentration equation:

$$\frac{\partial C}{\partial t}+v\frac{\partial C}{\partial y}=D_{MY}\frac{\partial^2 C}{\partial y^2} \tag{5}$$

With initial and boundary conditions:

$$\begin{aligned}&(t\le 0)\ u=o\ \ w=o\ \ v=v_0\ \ T=T_w+\varepsilon\left(T_w-T_\infty\right)e^{i\omega t}\\ &C=C_w+\varepsilon\left(C_w-C_\infty\right)e^{i\omega t}\ \ \omega t=\frac{\pi}{2},\ \varepsilon=0.2\ \text{at}\ y=0\\ &(t>o)\ u\to o,\ w\to o,\ T\to T_\infty\ \ C\to C_\infty\ \text{As}\ y\to\infty\end{aligned} \tag{6}$$

The following non dimensional quantities are introduced,

$$y^*=\frac{y\ v_0}{\upsilon}\ \ t^*=\frac{tv_0^2}{4\upsilon}\ \ u^*=\frac{u}{v_0}\ \ \upsilon=\frac{\eta_0}{\rho}\ \ w^*=\frac{w}{v_0}$$

$$\omega^*=\frac{4\upsilon\omega}{v_0'^2}\ \ T^*=\frac{T-T_\infty}{T_w-T_\infty}\ \ C^*=\frac{C-C_\infty}{C_w-C_\infty}\ \ M=\frac{\sigma B_o^2}{\rho}\left(\frac{\upsilon}{v_0^{*2}}\right)$$

$$X_i=\frac{v_0^{*2}k_p}{\upsilon^2}\ \ G_r=\frac{\beta g\upsilon(T_w-T_\infty)}{v_0^{*3}}$$

$$G_c=\frac{\beta^* g\upsilon(C_w-C_\infty)}{v_0^{*3}}\ \ R_o=\frac{\Omega\upsilon}{v_0^{*2}}$$

$$P_r=\frac{\rho C_p\upsilon}{k}\ E_c=\frac{v_0^{*2}}{C_p\left(T_w-T_\infty\right)}\ S=\frac{Q_0\upsilon}{\rho C_p v_0^{*2}}\ S_c=\frac{\upsilon}{D} \tag{7}$$

Where, $g,\rho,\sigma,\upsilon,\beta,\beta^*,\omega,\eta_0,K_p,T,T_w,T_\infty,C,C_w,C_\infty,C_p,D_{MY}$ are acceleration due to gravity, density, electrical conductivity, coefficient of kinematic viscosity, volumetric coefficient of expansion for heat transfer, volumetric coefficient of expansion for mass transfer, angular frequency, coefficient of viscosity, thermal diffusivity at constant pressure, temperature, temperature at the plate, temperature at infinity, concentration, concentration at the plate, concentration at infinity, specific heat at constant pressure, molecular mass diffusivity respectively.

The governing equations in non-dimensional form are:

$$\frac{1}{4}\frac{\partial u^*}{\partial t^*}+\frac{\partial u^*}{\partial y^*}+2R_o w^*=\frac{\partial^2 u^*}{\partial y^{*2}}-\frac{1}{X_i}u^*-Mu^*+Gr_\theta T^*+Gr_c C^* \tag{8}$$

$$\frac{1}{4}\frac{\partial w^*}{\partial t^*}+\frac{\partial w^*}{\partial y^*}-2R_o u^*=\frac{\partial^2 w^*}{\partial y^{*2}}-\frac{1}{X_i}w^*-Mw^* \tag{9}$$

$$\frac{1}{4}\frac{\partial T^*}{\partial t^*}+\frac{\partial T^*}{\partial y^*}=\frac{1}{p_r}\frac{\partial^2 T^*}{\partial y^{*2}}+E_c\left(\frac{\partial u^*}{\partial y^*}\right)^2+ST^* \tag{10}$$

$$\frac{1}{4}\frac{\partial C^*}{\partial t^*}+\frac{\partial C^*}{\partial y^*}=\frac{1}{S_c}\frac{\partial^2 C^*}{\partial y^{*2}} \tag{11}$$

With initial and boundary conditions as,

$$\begin{cases}(t\le 0)\ u^*=o,\ w^*=o,\ T^*=1+\varepsilon e^{i\omega t},\ C^*=1+\varepsilon e^{i\omega t}\\ \omega t=\dfrac{\pi}{2},\ \varepsilon=0.2\ \text{at}\ y^*=0\\ (t>o)\ \ u^*\to 0\ C^*\to 0\ \text{As}\ y^*\to\infty\end{cases} \tag{12}$$

3. Method of Solution

The set of differential equations (8) – (11) subject to the boundary conditions (12), are highly nonlinear, coupled and therefore they cannot be solved analytically. Hence, the Crank-Nicolson method is used to obtain an accurate and efficient solution to the boundary value problem under consideration. Setting the finite difference averages for velocity, temperature and concentration as:

$$u^*=\frac{U_{i,j+1}+U_{i,j}}{2}$$

$$\frac{\partial u^*}{\partial t^*}=\frac{U_{i,j+1}-U_{i,j}}{\Delta t}$$

$$\frac{\partial u^*}{\partial y^*}=\frac{U_{i+1,j+1}-U_{i-1,j+1}+U_{i+1,j}-U_{i-1,j}}{4\Delta y} \tag{13}$$

$$\frac{\partial^2 u^*}{\partial y^{*2}}=\frac{U_{i-1,j+1}-2U_{i,j+1}+U_{i+1,j+1}+U_{i-1,j}-2U_{i,j}+U_{i+1,j}}{2(\Delta y)^2}$$

$$T^*=\frac{T_{i,j+1}+T_{i,j}}{2}$$

$$\frac{\partial T^*}{\partial t^*}=\frac{T_{i,j+1}-T_{i,j}}{\Delta t}$$

$$\frac{\partial T^*}{\partial y^*}=\frac{T_{i+1,j+1}-T_{i-1,j+1}+T_{i+1,j}-T_{i-1,j}}{4\Delta y}$$

$$\frac{\partial^2 T^*}{\partial y^{*2}}=\frac{T_{i-1,j}-2T_{i,j}+T_{i+1,j}+T_{i-1,j+1}-2T_{i,j+1}+T_{i+1,j+1}}{2(\Delta y)^2} \tag{14}$$

$$\frac{\partial C^*}{\partial t^*}=\frac{C_{i,j+1}-C_{i,j}}{\Delta t}$$

$$\frac{\partial C^*}{\partial y^*}=\frac{C_{i+1,j+1}-C_{i-1,j+1}+C_{i+1,j}-C_{i-1,j}}{4\Delta y}$$

$$\frac{\partial^2 C^*}{\partial y^{*2}}=\frac{C_{i-1,j}-2C_{i,j}+C_{i+1,j}+C_{i-1,j+1}-2C_{i,j+1}+C_{i+1,j+1}}{2(\Delta y)^2} \tag{15}$$

We Substitute (13), (14) and (15) in equations (8) to (11). Equation (8) becomes,

$$U_{i-1,j+1}\left(\frac{-\Delta t\Delta yX_i-2\Delta tX_i}{4\Delta t\Delta y^2X_i}\right)+U_{i,j+1}\left(\frac{X_i\Delta y^2+4\Delta tX_i+2\Delta t\Delta y^2+2M\Delta t\Delta y^2X_i}{4\Delta t\Delta y^2X_i}\right)+U_{i+1,j+1}\left(\frac{\Delta t\Delta yX_i-2\Delta tX_i}{4\Delta t\Delta y^2X_i}\right)=$$
$$U_{i-1,j}\left(\frac{\Delta t\Delta yX_i+2\Delta tX_i}{4\Delta t\Delta y^2X_i}\right)+U_{i,j}\left(\frac{\Delta y^2X_i-4\Delta tX_i-2\Delta t\Delta y^2-2M\Delta t\Delta y^2X_i}{4\Delta t\Delta y^2X_i}\right)+U_{i+1,j}\left(\frac{-\Delta t\Delta yX_i+2\Delta tX_i}{4\Delta t\Delta y^2X_i}\right) \quad (16)$$
$$-2R_0w+G_{r\theta}T+G_{rc}C$$

Multiplying all through by $4\Delta t\Delta y^2X_i$ simplifying, and letting the coefficients of interior nodes to be:

$$a_i=-\Delta t\Delta yX_i-2\Delta tX_i$$

$$b_i=X_i\Delta y^2+4\Delta tX_i+2\Delta t\Delta y^2+2M\Delta t\Delta y^2X_i$$

$$c_i=\Delta t\Delta yX_i-2\Delta tX_i$$

$$d_i=U_{i-1,j}\left(\Delta t\Delta yX_i+2\Delta tX_i\right)$$

$$e_i=U_{i,j}\left(\Delta y^2X_i-4\Delta tX_i-2\Delta t\Delta y^2-2M\Delta t\Delta y^2X_i\right)$$

$$f_i=U_{i+1,j}\left(-\Delta t\Delta yX_i+2\Delta tX_i\right)$$

$$g=-2R_0w\left(4\Delta t\Delta y^2X_i\right)+G_{r\theta}T\left(4\Delta t\Delta y^2X_i\right)+G_{rc}C\left(4\Delta t\Delta y^2X_i\right) \quad (17)$$

We have,

$$a_iU_{i-1,j+1}+b_iU_{i,j+1}+c_iU_{i+1,j+1}=d_i+e_i+f_i+g \quad (18)$$

Equation (18) can be represented in a tridiagonal matrix form as follows. For i=2, 3, 4….. (N-1)

$$\begin{bmatrix} a_2 & b_2 & c_2 & 0 & 0 & 0 & 0\\ 0 & a_3 & b_3 & c_3 & \ddots & 0 & 0\\ 0 & 0 & \ddots & \ddots & \ddots & \ddots & 0\\ 0 & 0 & 0 & \ddots & \ddots & \ddots & \ddots\\ 0 & 0 & 0 & 0 & a_{N-1} & b_{N-1} & c_{N-1} \end{bmatrix}\begin{bmatrix} u_{1,j+1}\\ u_{2,j+1}\\ \vdots\\ u_{3,j+1} \end{bmatrix}=\begin{bmatrix} d_2\\ d_3\\ \vdots\\ d_{N+1} \end{bmatrix}+\begin{bmatrix} e_2\\ e_3\\ \vdots\\ e_{N+1} \end{bmatrix}+\begin{bmatrix} f_2\\ f_3\\ \vdots\\ f_{N+1} \end{bmatrix}+\begin{bmatrix} g\\ g\\ \vdots\\ g \end{bmatrix} \quad (19)$$

Equation (9) becomes,

$$W_{i-1,j+1}\left(\frac{-\Delta t\Delta yX_i-2\Delta tX_i}{4\Delta t\Delta y^2X_i}\right)+W_{i,j+1}\left(\frac{X_i\Delta y^2+4\Delta tX_i+2\Delta t\Delta y^2+2M\Delta t\Delta y^2X_i}{4\Delta t\Delta y^2X_i}\right)+W_{i+1,j+1}\left(\frac{\Delta t\Delta yX_i-2\Delta tX_i}{4\Delta t\Delta y^2X_i}\right)=$$
$$W_{i-1,j}\left(\frac{\Delta t\Delta yX_i+2\Delta tX_i}{4\Delta t\Delta y^2X_i}\right)+W_{i,j}\left(\frac{\Delta y^2X_i-4\Delta tX_i-2\Delta t\Delta y^2-2M\Delta t\Delta y^2X_i}{4\Delta t\Delta y^2X_i}\right)+W_{i+1,j}\left(\frac{-\Delta t\Delta yX_i+2\Delta tX_i}{4\Delta t\Delta y^2X_i}\right)+2R_ou \quad (20)$$

Multiplying all through by $4\Delta t\Delta y^2X_i$ simplifying, and letting the coefficients of interior nodes to be:

$$a_i=-\Delta t\Delta yX_i-2\Delta tX_i$$

$$b_i=X_i\Delta y^2+4\Delta tX_i+2\Delta t\Delta y^2+2M\Delta t\Delta y^2X_i$$

$$c_i=\Delta t\Delta yX_i-2\Delta tX_i$$

$$d_i = W_{i-1,j}\left(\Delta t\Delta y X_i + 2\Delta t X_i\right)$$

$$e_i = W_{i,j}\left(\Delta y^2 X_i - 4\Delta t X_i - 2\Delta t\Delta y^2 - 2M\Delta t\Delta y^2 X_i\right)$$

$$f_i = W_{i+1,j}\left(-\Delta t\Delta y X_i + 2\Delta t X_i\right)$$

$$g = 2R_0 u\left(4\Delta t\Delta y^2 X_i\right) \tag{21}$$

We have,

$$a_i W_{i-1,j+1} + b_i W_{i,j+1} + c_i W_{i+1,j+1} = d_i + e_i + f_i + g \tag{22}$$

Equation (22) can be represented in a tridiagonal matrix form as follows. For i=2, 3, 4….. (N-1)

$$\begin{bmatrix} a_2 & b_2 & c_2 & 0 & 0 & 0 & 0 \\ 0 & a_3 & b_3 & c_3 & \ddots & 0 & 0 \\ 0 & 0 & \ddots & \ddots & \ddots & \ddots & 0 \\ 0 & 0 & 0 & \ddots & \ddots & \ddots & \ddots \\ 0 & 0 & 0 & 0 & a_{N-1} & b_{N-1} & c_{N-1} \end{bmatrix} \begin{bmatrix} w_{1,j+1} \\ w_{2,j+1} \\ \vdots \\ w_{3,j+1} \end{bmatrix} = \begin{bmatrix} d_2 \\ d_3 \\ \vdots \\ d_{N+1} \end{bmatrix} + \begin{bmatrix} e_2 \\ e_3 \\ \vdots \\ e_{N+1} \end{bmatrix} + \begin{bmatrix} f_2 \\ f_3 \\ \vdots \\ f_{N+1} \end{bmatrix} + \begin{bmatrix} g \\ g \\ \vdots \\ g \end{bmatrix} \tag{23}$$

Equation (10) becomes:

$$\begin{aligned} &T_{i-1,j+1}\left(\frac{-\Delta t\Delta y P_r - 2\Delta t}{4P_r\Delta t\Delta y^2}\right) + T_{i,j+1}\left(\frac{P_r\Delta y^2 + 4\Delta t - 2P_r\Delta t\Delta y^2 S}{4P_r\Delta t\Delta y^2}\right) + T_{i+1,j+1}\left(\frac{\Delta t\Delta y P_r - 2\Delta t}{4P_r\Delta t\Delta y^2}\right) = \\ &T_{i,j}\left(\frac{P_r\Delta y^2 - 4\Delta t + 2P_r S\Delta t\Delta y^2}{4P_r\Delta t\Delta y^2}\right) + T_{i+1,j}\left(\frac{-P_r\Delta t\Delta y + 2\Delta t}{4P_r\Delta t\Delta y^2}\right) + T_{i-1,j}\left(\frac{P_r\Delta t\Delta y + 2\Delta t}{4P_r\Delta t\Delta y^2}\right) + E_c\left(U_y\right)^2 \end{aligned} \tag{24}$$

Multiplying all through by $4P_r\Delta t\Delta y^2$ simplifying, and letting the coefficients of interior nodes to be:

$$a_i = -\Delta t\Delta y P_r - 2\Delta t$$

$$b_i = P_r\Delta y^2 + 4\Delta t - 2P_r\Delta t\Delta y^2 S$$

$$c_i = \Delta t\Delta y P_r - 2\Delta t$$

$$d_i = T_{i,j}\left(P_r\Delta y^2 - 4\Delta t + 2P_r S\Delta t\Delta y^2\right)$$

$$e_i = T_{i+1,j}\left(-P_r\Delta t\Delta y + 2\Delta t\right)$$

$$f_i = T_{i-1,j}\left(P_r\Delta t\Delta y + 2\Delta t\right)$$

$$g = 4E_c\left(U_y\right)^2 P_r\Delta t\Delta y^2 \tag{25}$$

We have,

$$a_i T_{i-1,j+1} + b_i T_{i,j+1} + c_i T_{i+1,j+1} = d_i + e_i + f_i + g \tag{26}$$

Equation (26) can be represented in a tridiagonal matrix form as follows. For i=2, 3, 4….. (N-1)

$$\begin{bmatrix} a_2 & b_2 & c_2 & 0 & 0 & 0 & 0 \\ 0 & a_3 & b_3 & c_3 & \ddots & 0 & 0 \\ 0 & 0 & \ddots & \ddots & \ddots & \ddots & 0 \\ 0 & 0 & 0 & \ddots & \ddots & \ddots & \ddots \\ 0 & 0 & 0 & 0 & a_{N-1} & b_{N-1} & c_{N-1} \end{bmatrix} \begin{bmatrix} T_{1,j+1} \\ T_{2,j+1} \\ \vdots \\ T_{3,j+1} \end{bmatrix} = \begin{bmatrix} d_2 \\ d_3 \\ \vdots \\ d_{N+1} \end{bmatrix} + \begin{bmatrix} e_2 \\ e_3 \\ \vdots \\ e_{N+1} \end{bmatrix} + \begin{bmatrix} f_2 \\ f_3 \\ \vdots \\ f_{N+1} \end{bmatrix} + \begin{bmatrix} g \\ g \\ \vdots \\ g \end{bmatrix} \tag{27}$$

Equation (11) becomes:

$$\begin{aligned} &C_{i-1,j+1}\left(\frac{-\Delta t\Delta y S_c - 2\Delta t}{4\Delta t\Delta y^2 S_c}\right) + C_{i,j+1}\left(\frac{S_c\Delta y^2 + 4\Delta t}{4\Delta t\Delta y^2 S_c}\right) + C_{i+1,j+1}\left(\frac{S_c\Delta t\Delta y - 2\Delta t}{4\Delta t\Delta y^2 S_c}\right) = \\ &C_{i-1,j}\left(\frac{S_c\Delta y\Delta t + \Delta t}{4\Delta t\Delta y^2 S_c}\right) + C_{i,j}\left(\frac{S_c\Delta y^2 - 4\Delta t}{4\Delta t\Delta y^2 S_c}\right) + C_{i+1,j}\left(\frac{-S_c\Delta t\Delta y + 2\Delta t}{4\Delta t\Delta y^2 S_c}\right) \end{aligned} \tag{28}$$

Multiplying all through by $4\Delta t\Delta y^2 S_c$ simplifying, and letting the coefficients of interior nodes to be:

$$\begin{aligned} a_i &= -\Delta t\Delta y S_c - 2\Delta t \\ b_i &= S_c\Delta y^2 + 4\Delta t \\ c_i &= S_c\Delta t\Delta y - 2\Delta t \\ d_i &= C_{i-1,j}\left(S_c\Delta y\Delta t + \Delta t\right) \\ e_i &= C_{i,j}\left(S_c\Delta y^2 - 4\Delta t\right) \\ f_i &= C_{i+1,j}\left(-S_c\Delta t\Delta y + 2\Delta t\right) \end{aligned} \tag{29}$$

We have,

$$a_i C_{i-1,j+1} + b_i C_{i,j+1} + c_i C_{i+1,j+1} = d_i + e_i + f_i \tag{30}$$

Equation (30) can be represented in a tridiagonal matrix form as follows. For i=2, 3, 4….. (N-1)

$$\begin{bmatrix} a_2 & b_2 & c_2 & 0 & 0 & 0 & 0 \\ 0 & a_3 & b_3 & c_3 & \ddots & 0 & 0 \\ 0 & 0 & \ddots & \ddots & \ddots & \ddots & 0 \\ 0 & 0 & 0 & \ddots & \ddots & \ddots & \ddots \\ 0 & 0 & 0 & 0 & a_{N-1} & b_{N-1} & c_{N-1} \end{bmatrix} \begin{bmatrix} C_{1,j+1} \\ C_{2,j+1} \\ \vdots \\ C_{3,j+1} \end{bmatrix} = \begin{bmatrix} d_2 \\ d_3 \\ \vdots \\ d_{N+1} \end{bmatrix} + \begin{bmatrix} e_2 \\ e_3 \\ \vdots \\ e_{N+1} \end{bmatrix} + \begin{bmatrix} f_2 \\ f_3 \\ \vdots \\ f_{N+1} \end{bmatrix} \tag{31}$$

Matrices (19), (23), (27) and (31) are simulated using MATLAB algorithm subject to initial and boundary conditions (12)

4. Results and Discussions

The effect of Mass transfer on unsteady free convective flow of a viscous incompressible electrically conducting fluid past an infinite vertical rotating porous plate with constant injection and heat source in presence of a transverse magnetic field has been studied. The governing equations of the flow problem have been solved using Finite Difference Method. The effects of the flow parameters are analyzed and discussed with the help of velocity profiles, temperature profiles and concentration distribution. During numerical calculations we have chosen the values of Pr =0.71 representing air at 25°C, Sc =0.60 representing H2O vapor, Grc>0 corresponding to cooling of the plate and S>0 representing heat source. The figures below represent effects of variation of various parameters on velocity, temperature and concentration profiles. The block lines represent primary velocity profiles while the broken lines represent secondary velocity profiles.

Velocity Profiles

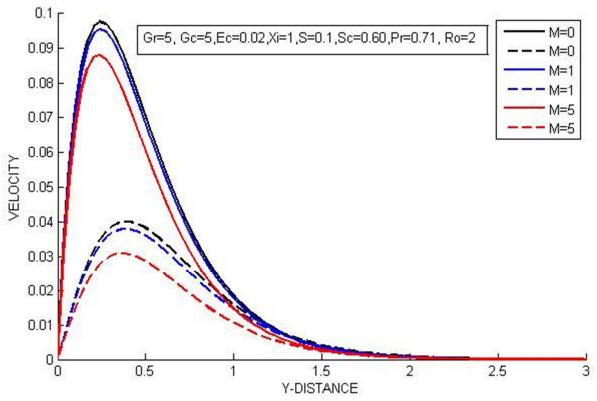

Fig. 2. *Velocity profiles for different values of Hartmann number (M).*

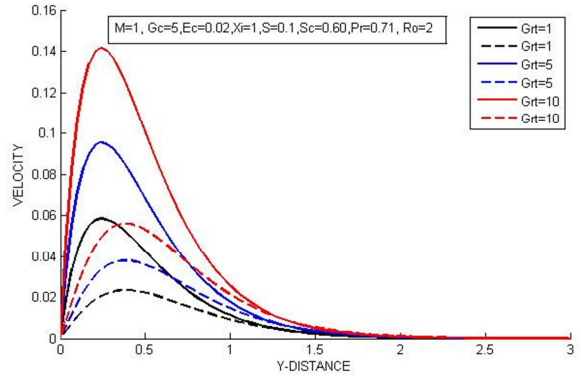

Fig. 3. *Velocity profiles for different values of Grc.*

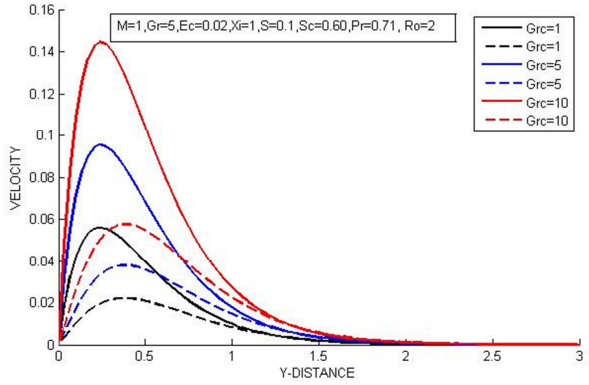

Fig. 4. *Velocity profiles for different values of Grt.*

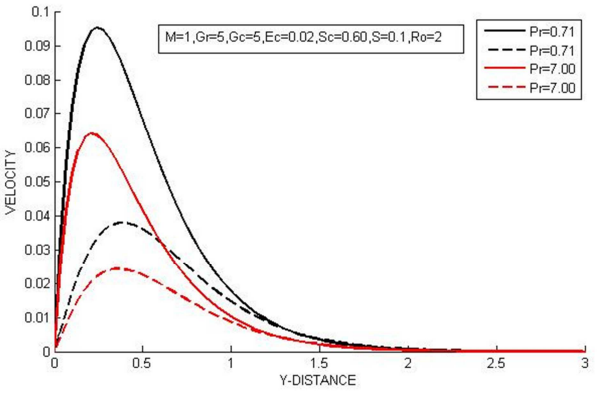

Fig. 5. *Velocity profiles for different values of P_r.*

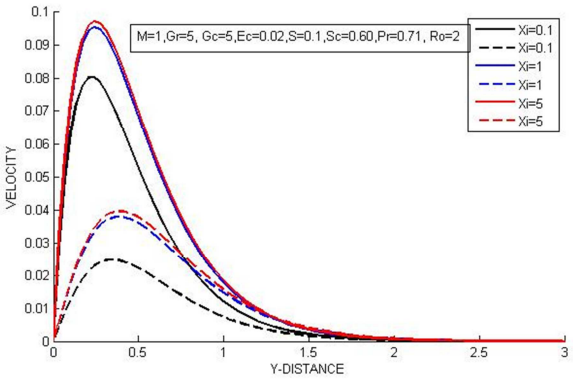

Fig. 6. *Velocity profiles for different values of X.*

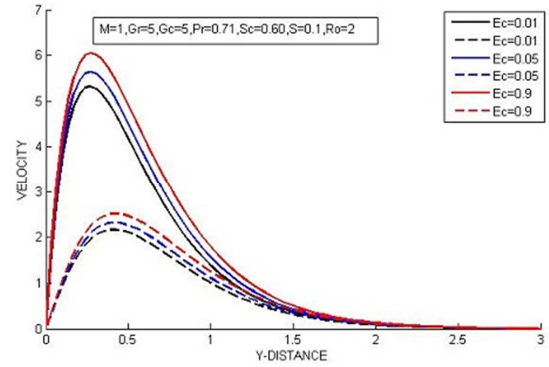

Fig. 7. *Velocity profiles for different values of E_c.*

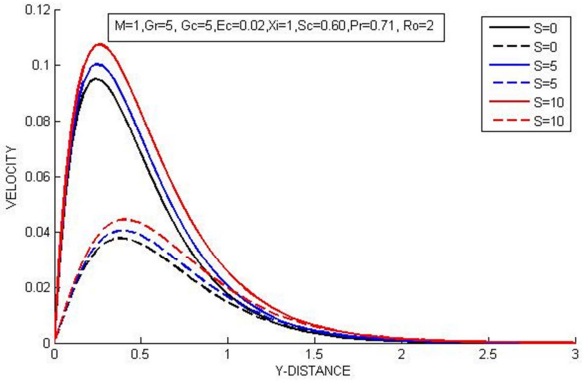

Fig. 8. *Velocity profiles for different values of S.*

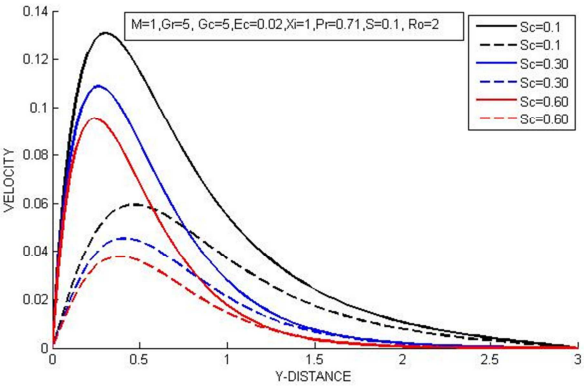

Fig. 9. *Velocity profiles for different values of S_c.*

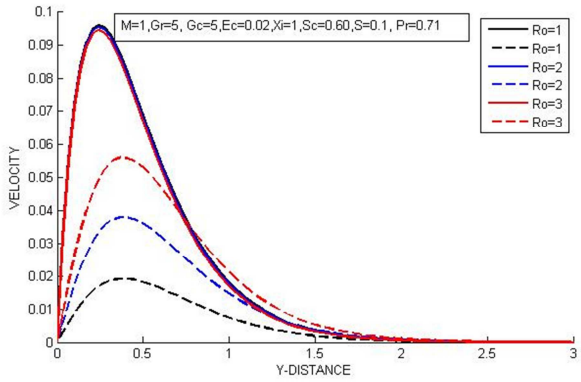

Fig. 10. *Velocity profiles for different values of R_0.*

Temperature Profiles

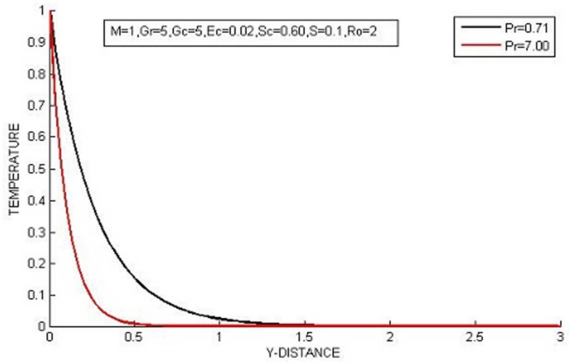

Fig. 11. *Temperature profiles for different values of P_r.*

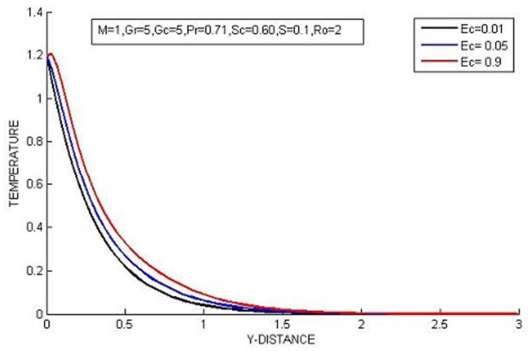

Fig. 12. *Temperature profiles for different values of E_c.*

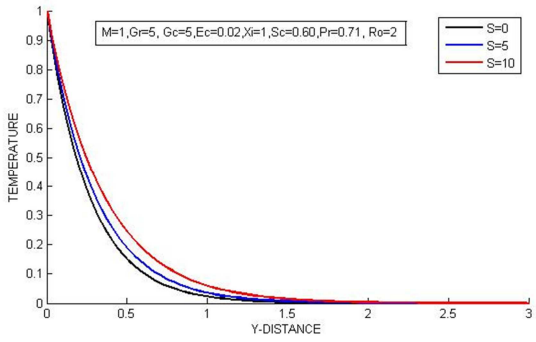

Fig. 13. *Temperature profiles for different values of S.*

Concentration Profiles

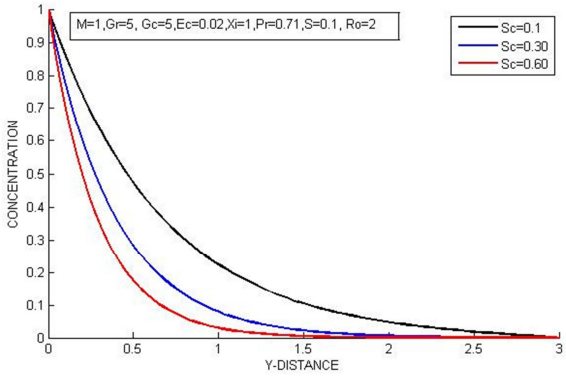

Fig. 14. *Concentration profiles for different values of S_c.*

From Fig. 2, it is observed that, an increase in Hartmann number M, leads to a decrease in both the primary and secondary velocity. This is because when M increases it means that, electromagnetic force increases and when transverse magnetic field is applied to an electrically conducting fluid, it gives rise to a force called the Lorentz force which acts against the flow if applied in the normal direction as in the present study. This resistive force has a tendency to slow down the motion of the fluid in the boundary layer. A weak magnetic field does not have much effect on velocity. When M = 0 means that magnetic force is so small compared to viscous force.

From Fig. 3 increase in the Grashof number for heat transfer G_{rt} , causes an increase in the primary velocity profiles and an increase in the magnitude of the secondary velocity profiles respectively. The Grashof number for heat transfer G_{rt} represents the effects of free convection currents and physically $G_{rt} > 0$ corresponds to heating of the fluid (or cooling of the surface). Velocity of the fluid increases because the fluid flow is assisted by the free convection currents. As expected, increase in the velocity profiles is partly due to the enhancement of thermal buoyancy force.

Fig. 4 shows that increase in Grashof number for mass transfer G_{rc} causes an increase in the primary velocity profiles. It also causes increase in the magnitude of the secondary velocity profiles. The velocity distribution attains a distinctive maximum value near the porous plate and then decays smoothly to approach a free stream value. The Grashof number for mass transfer G_{rc} defines the ratio of the species buoyancy force to the viscous hydrodynamic force hence, as expected, the fluid velocity increases due to increase in the species buoyancy force. Increase in species buoyancy force results into a higher species transportation rate away from the rotating plate, resulting into lower concentration.

Fig. 5 shows the effect of the Prandtl number on both primary and secondary velocity profiles. The values of the Prandtl number are chosen Air at 25^0c and one atmospheric pressure (P_r = 0.71), and water at 25^0c (P_r = 7.00). It is observed that increasing the values of the Prandtl number, results in a decrease in the fluid velocity. This is because, an increase in Prandtl number means that the viscous forces are

increasing as the thermal forces increase hence decreasing the velocity of the fluid particles.

Fig. 6 shows that increase in permeability parameter X_i causes an increase in both the primary and secondary velocity profiles. It is observed that the fluid velocity increases and a peak value is attained near the plate then decays continuously to approach the free stream. Increasing X_i decreases the resistance of the porous medium since permeability physically becomes more with an increase in X_i. This increases the magnitude of the flow velocity.

Fig. 7 shows that increase in Eckert number E_c, causes an increase in both the primary and secondary velocity profiles. It is observed that the fluid velocity increases sharply and obtains a distinctive maximum value near to the wall of the porous plate and then decays continuously with increasing y distance. This is because when E_c is large, it implies that the kinetic energy dominates the boundary layer enthalpy which means that the particles or molecules of the fluid have high velocities. When the Ec number is small, it implies that the kinetic energy is small and hence the particles have low velocities, hence when E_c is increased, the velocity also increases.

Fig. 8 shows the primary and secondary velocity profiles for different values of heat source S. It is observed that an increase in the heat source parameter S, results to an increase in the fluid velocity. The presence of a heat source produces a heating effect that increase velocity of the convection currents that move next to the surface of the rotating plate, leading to higher velocity profiles.

Fig. 9 shows that increase in Schmidt number S_c causes a decrease in primary profiles and in the magnitude of the secondary velocity profiles respectively. The values of S_c are chosen for the gases so that: Hydrogen ($S_c = 0.1$), Helium (S_c=0.30), Water vapor (S_c=0.60). The Schmidt number S_c signifies the ratio of the momentum to mass diffusivity. It quantifies the relative effectiveness of momentum and mass transport by diffusion in the hydrodynamic (velocity) and concentration (species) boundary layers. An increase in S_c leads to thinning of the velocity and the concentration boundary layers respectively. A large value of S_c means a presence of a heavier fluid and this implies a lower velocity of the fluid.

Fig. 10 shows that that as rotation parameter R_o increases; the primary velocity u decreases whereas secondary velocity w increases. This indicates that rotation retards fluid flow in the primary flow direction, but it accelerates fluid flow in the secondary flow direction. This is due to the fact that the Coriolis force acts as a constraint in the main fluid flow when the plate is suddenly set into motion. It can be said that Coriolis force ends fluid flow in the primary flow direction to induce cross flow and secondary flow in the flow field. Absence of rotation translates to absence of the secondary velocity profiles. This means rotation can be used to control emergence of the secondary velocity profiles in a rotating system.

The temperature of the flow suffers a substantial change with the variation of the flow parameters such as Prandtl number P_r, Eckert number E_c and Heat source parameter S. The temperature profiles are in good agreement with those of Das et al. (2010). From fig. 11, it is observed that an increase in Prandtl Number leads to a decrease in temperature profiles. This is because the viscous forces dominate over thermal forces as Prandtl Number is raised. An increase in the Prandtl Number results to a decrease of the thermal boundary layer thickness and in general lowers the average temperature in the boundary layer. Smaller values of P_r are equivalent to increase in the thermal conductivity of the fluid and therefore heat is able to diffuse away from the heated surface more rapidly than for higher values of P_r. Thus, the temperature of water at 25^0c (P_r = 7.00) falls more rapidly compared to Air at 25^0c and one atmospheric pressure (P_r = 0.71). Prandtl number controls the relative thickness of the momentum and thermal boundary layers.

Fig. 12 shows that an increase in Eckert number E_c leads to an increase in temperature profiles. Hence the rate at which the fluid loses heat decreases as the Eckert Number is increased. This observation can be attributed to the viscous dissipation which increases with kinetic energy of the fluid particles. Increase in E_c means the fluid absorbs more heat energy that is released from the internal viscous forces. This in turn increases the temperature of the convection currents due to increased thermal buoyancy forces.

Fig. 13 shows the variation of different values of the heat source parameter to the temperature. It is observed that as S increases, the temperature increase. Increase in heat source produces a heating effect hence increase in the temperature. The thermal boundary layer is weakened when heat source is present hence the increase in temperature.

Fig. 14 shows that an increase in Schmidt number Sc causes decrease in the concentration of the fluid. The values of S_c are chosen for the gases so that: Hydrogen (S_c=0.1), Helium (S_c=0.30) and Water vapor (S_c=0.60). The concentration falls gradually and progressively for hydrogen in distinction to other gases. This is because an increase of S_c mean a decrease of molecular diffusivity, which results in decrease of concentration boundary layer. Hence, the concentration of species is smaller for higher values of S_c.

5. Conclusion

A summary of effects of varying different flow parameters on the velocity, temperature and the concentration distribution of the flow is given below

1. An increase in Hartmann's number M, Prandtl number P_r and Schmidt number S_c retards both the primary and secondary velocity of the fluid at all points.
2. The effect of increasing Grashof number for heat transfer G_{rt}, Grashof number for mass transfer G_{rc}, permeability parameter X_i, Heat source parameter S,

and Eckert number E_c is to accelerate both the primary and secondary velocity profiles at all points.

3. Rotation parameter R_o retards fluid flow in the primary flow direction, but it accelerates fluid flow in the secondary flow direction. Absence of rotation translates to absence of the secondary velocity profiles. This means rotation can be used to control emergence of the secondary velocity profiles in a rotating system.
4. An increase in Eckert number E_c and heat source parameter S, increases the temperature of the flow field at all points while a growing Prandtl number P_r retards the temperature of the flow. The temperature of the flow grows rapidly for small values ($P_r < 1$) and for higher values the effect reverses.
5. The effect of increasing Schmidt number S_c is to reduce the concentration boundary layer thickness of the flow field at all points. The concentration of species is smaller for higher values of S_c.

References

[1] Das, S., & Mitra, M. (2009). Unsteady mixed convective MHD flow and mass transfer past an accelerated infinite vertical plate with suction. *Ind. J. Sci. Tech*, *2 (5)*, 18-22.

[2] Das, S., A. Satapathy, J., Das, & Panda, J. (2009). Mass transfer effects on MHD flow and heat transfer past a vertical porous plate through a porous medium under oscillatory suction and heat source. *International Journal of Heat and Mass Transfer*, *52*, 5962-5969.

[3] Das, S., A. Satapathy, J., Das, &Sahoo, S. (2007). Numerical solution of unsteady free convective MHD flow past an accelerated vertical plate with suction and heat flux. *J. Ultra Sci. Phys. Sci*, *19(1)*, 105-112.

[4] Das, S., Sahoo, S., & Dash, G. (2006). Numerical solution of mass transfer effects on unsteady flow past an accelerated vertical porous plate with suction. *Bulletin of the Malayssian Mathematical Sciences Society*, *29(1)*, 33-42.

[5] Das, S., Tripathy, U., & Das, J. (2010). Hydromagnetic convective flow past a vertical porous plate through a porous medium with suction and heat source. *International Journal of Energy and Environment*, *1(3)*, 467-478.

[6] Elbasheshy, E., Yassmin, D., & Dalia, A. (2010). Heat transfer over an unsteady porous stretching surface embedded in a porous medium with variable heat flux in the presence of heat source or sink. *African Journal of Mathematics and Computer Science research*, *3 (5)*, 68-73.

[7] Ferdows, M., Koji, K., & Chien-Hsin, C. (2010). Dufour, soret and viscous dissipation effects on heat and mass transfer in porous media with high porosities. *International Journal of Applied Engineering Research*, *5 (3)*, 477-484.

[8] Kang'ethe, G., Kinyanjui, M. N., & Uppal, S. M. (2012). MHD Flow In Porous Media Over A Stretching Surface In A Rotating System With Heat And Mass Transfer. *International Electronic Journal of Pure and Applied Mathematics*, *4* (1), 9-32.

[9] Kinyanjui, M., Chartuvedi, N., & Uppal, S. (1998). MHD Stokes problem for a vertical infinite plate in a dissipative rotating fluid with Hall current. *Journal of Magnetohydrodynamic and plasma research*, *8* (No 1), pp 15-30.

[10] Makinde, O., Mango, J., & Theuri, D. (2003). Unsteady free convection flow with suction on an accelerating porous plate. *AMSE J. Mod. Meas*, *B 72 (3)*, 39-46.

[11] Naser, S., & Elgazery. (2008). Transient Analysis of Heat and Mass Transfer by Convection in Power-law fluid past a vertical plate immersed in a porous medium. *Application and Applied mathematics: An International Journal*, *3(2)*, 267-285.

[12] Rafael, C. (2005). Flow and heat transfer of a fluid through a porous medium over a stretching surface with internal heat generation/absorption and suction/blowing. *Fluid Dynamics Research*, *37*, 231-245.

[13] Subhas, A. M., Sujit, K., & Prasad. (2001). Convective heat and mass transfer in a visco-elastic fluid flow through a porous medium over a stretching sheet. *International Journal of Numerical Methods for Heat and Fluid Flow*, *11 (8)*, 779-792.

[14] Tamana, S., Sumon, S. M., & Goutam. (2009). Heat transfer in a porous medium over a stretching surface with internal heat generation and suction or injection in the presence of radiation. *Journal of Mechanical Engineering*, *40 (1)*, 22-28.